

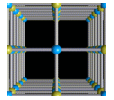
Convergence results for finite element and finite difference approximation of nonlocal fracture models

Prashant K. Jha

prashant.j16o@gmail.com
jha@math.lsu.edu

Joint work with
Dr. Robert Lipton

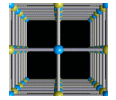
Funded by
Army Research Office



Outline of talk

1

- Peridynamic: Introduction
- Finite difference approximation and results
- Finite element approximation and results
- Summary and future works



Introduction

2

Let D be the material domain, D_c be nonlocal boundary, and \mathbf{u} be the displacement field.

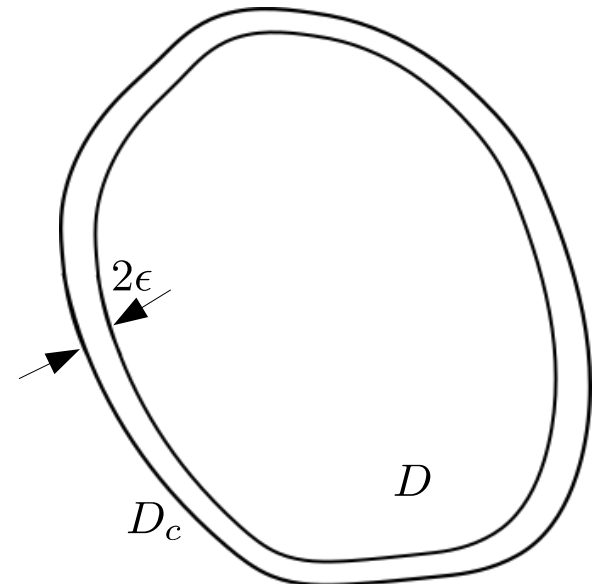
Let \mathbf{x} denote the material point and $\chi(\mathbf{x}) = \mathbf{x} + \mathbf{u}(\mathbf{x})$ denote the deformed position.

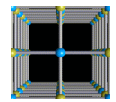
Strain between two material point \mathbf{x} and \mathbf{y} is given by

$$S(\mathbf{y}, \mathbf{x}; \mathbf{u}) = \frac{|\mathbf{y} + \mathbf{u}(\mathbf{y}) - \mathbf{x} - \mathbf{u}(\mathbf{x})| - |\mathbf{y} - \mathbf{x}|}{|\mathbf{y} - \mathbf{x}|}$$

Assuming that displacement is small compared to the size of material, we linearize S and get

$$S(\mathbf{y}, \mathbf{x}; \mathbf{u}) = \frac{\mathbf{u}(\mathbf{y}) - \mathbf{u}(\mathbf{x})}{|\mathbf{y} - \mathbf{x}|} \cdot \frac{\mathbf{y} - \mathbf{x}}{|\mathbf{y} - \mathbf{x}|}$$





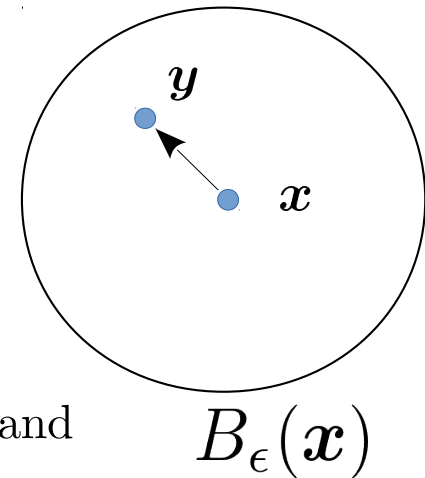
Neighborhood of material point

3

Consider a material point \mathbf{x} . We introduce a length scale ϵ which is called size of horizon. This controls the extent of nonlocal interaction in the material.

Hydrostatic strain (average strain) at material point \mathbf{x} is expressed as

$$\theta(\mathbf{x}; \mathbf{u}) = \frac{1}{|B_\epsilon(\mathbf{0})|} \int_{B_\epsilon(\mathbf{x})} J^\epsilon(|\mathbf{y} - \mathbf{x}|) S(\mathbf{y}, \mathbf{x}; \mathbf{u}) |\mathbf{y} - \mathbf{x}| d\mathbf{y}$$

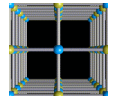


$J^\epsilon(|\mathbf{y} - \mathbf{x}|)$ is the influence function. We assume $J^\epsilon(|\mathbf{y} - \mathbf{x}|) = J(|\mathbf{y} - \mathbf{x}|/\epsilon)$ and function J satisfies $0 \leq J(r) \leq M$ for $r < 1$ and $J(r) = 0$ for $r \geq 1$.

Generic form of force at \mathbf{x} in peridynamic model is given by

$$\mathbf{F}^\epsilon(\mathbf{x}; \mathbf{u}) = \frac{1}{|B_\epsilon(\mathbf{x})|} \int_{B_\epsilon(\mathbf{x})} \hat{\mathbf{f}}^\epsilon(\mathbf{y}, \mathbf{x}; \mathbf{u}) d\mathbf{y}$$

$\hat{\mathbf{f}}^\epsilon$ depends on choice of ϵ and includes force due to pairwise interaction and force due to volume deformation.



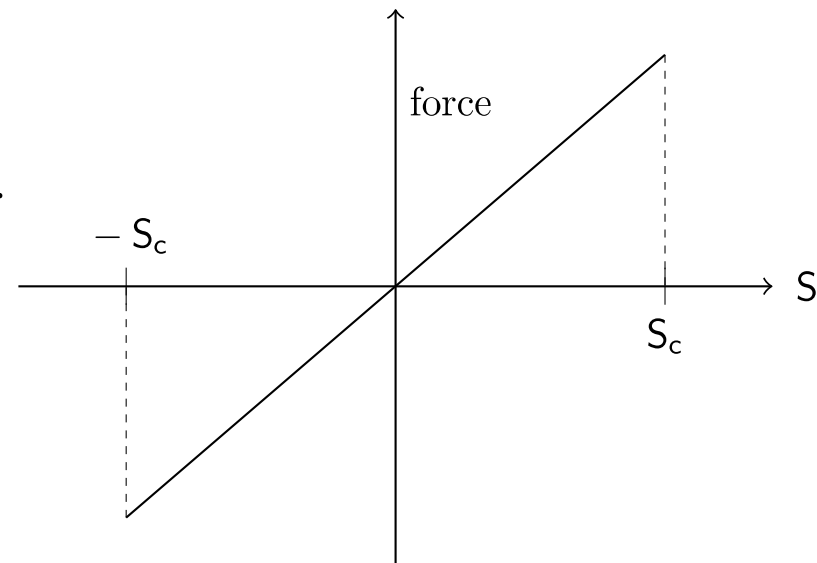
Example of pairwise force

4

- Example: Prototype Microelastic Brittle (PMB) material **Silling & Askari (2005), Bobaru & Hu (2012)**

$$\hat{\mathbf{f}}^\epsilon(\mathbf{y}, \mathbf{x}, \mathbf{u}) = \mu(S(\mathbf{y}, \mathbf{x}; \mathbf{u})) 4 \frac{J^\epsilon(|\mathbf{y} - \mathbf{x}|)}{\epsilon} S(\mathbf{y}, \mathbf{x}; \mathbf{u}) \frac{\mathbf{y} - \mathbf{x}}{|\mathbf{y} - \mathbf{x}|}$$

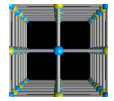
where $\mu(S) = 1$ if $|S| < S_c$ and $\mu(S) = 0$ when $|S| \geq S_c$.



- If $\mathbf{u} \in C^3(D; \mathbb{R}^d)$, and $\sup_{\mathbf{x} \in D} |\nabla^3 \mathbf{u}(\mathbf{x})| < \infty$ then

$$\sup_{x \in D} |\mathbf{f}^\epsilon(\mathbf{x}; \mathbf{u}) - \nabla \cdot \bar{\mathbb{C}} \mathcal{E} \mathbf{u}(\mathbf{x})| = O(\epsilon^2), \quad \bar{\mathbb{C}} = \frac{2}{|B_1(\mathbf{0})|} \int_{B_1(\mathbf{0})} J(|\boldsymbol{\xi}|) \mathbf{e}_\xi \otimes \mathbf{e}_\xi \otimes \mathbf{e}_\xi \otimes \mathbf{e}_\xi |\boldsymbol{\xi}| d\boldsymbol{\xi},$$

$\mathbf{e}_\xi = \boldsymbol{\xi}/|\boldsymbol{\xi}|$ and the strain tensor is $\mathcal{E} \mathbf{u}(\mathbf{x}) = (\nabla \mathbf{u}(\mathbf{x}) + \nabla \mathbf{u}^T(\mathbf{x}))/2$.



Regularized pairwise force

5

- We consider peridynamic force of the form **Lipton (2014)**

$$\mathbf{F}^\epsilon(\mathbf{x}; \mathbf{u}) = \frac{2}{|B_\epsilon(\mathbf{0})|} \int_{B_\epsilon(\mathbf{x})} \frac{J^\epsilon(|\mathbf{y} - \mathbf{x}|)}{\epsilon \sqrt{|\mathbf{y} - \mathbf{x}|}} \psi'(\sqrt{|\mathbf{y} - \mathbf{x}|} S) \frac{\mathbf{y} - \mathbf{x}}{|\mathbf{y} - \mathbf{x}|} d\mathbf{y}$$

Potential function ψ is multiwell function with one well at zero and other at $\pm \infty$

- Critical strain: $S_c^+(\mathbf{y}, \mathbf{x}) = \frac{r^+}{\sqrt{|\mathbf{y} - \mathbf{x}|}}$, $S_c^-(\mathbf{y}, \mathbf{x}) = \frac{r^-}{\sqrt{|\mathbf{y} - \mathbf{x}|}}$

- Example: $\psi(r) = c(1 - \exp[-\beta r^2])$

c, β are determined from elastic and fracture properties of material

$$r^+ = -r^- = \frac{1}{\sqrt{2\beta}}$$

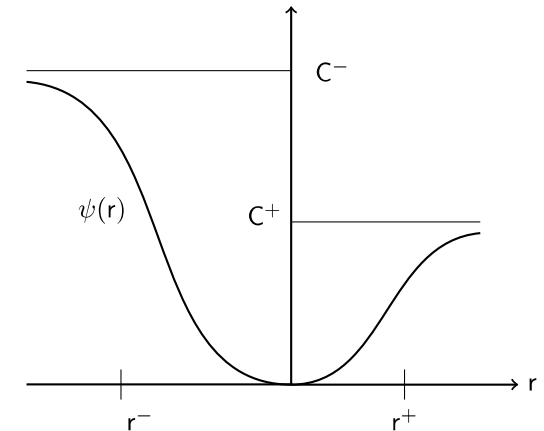


Fig: Profile of ψ

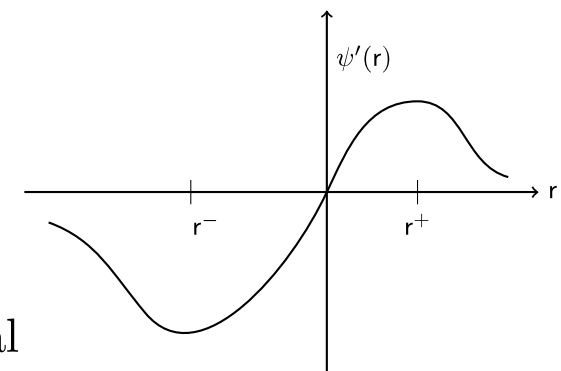
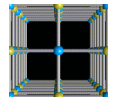


Fig: Profile of ψ'



State-based peridynamic force

6

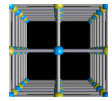
- We consider peridynamic force of the form **Lipton et al (2018)**

$$\mathbf{F}^\epsilon(\mathbf{x}; \mathbf{u}) = \frac{1}{|B_\epsilon(\mathbf{0})|} \int_{B_\epsilon(\mathbf{x})} \frac{J^\epsilon(|\mathbf{y} - \mathbf{x}|)}{\epsilon^2} (g'(\theta(\mathbf{y}; \mathbf{u})) + g'(\theta(\mathbf{x}; \mathbf{u}))) \frac{\mathbf{y} - \mathbf{x}}{|\mathbf{y} - \mathbf{x}|} d\mathbf{y}$$

Potential function g can either be multiwell function, similar to ψ , or it can be quadratic function giving linear force for hydrostatic strain θ

- Example: In this work we consider $g(r) = \bar{C}r^2/2$

\bar{C} is determined from elastic properties of material



Peridynamic energy and equation of motion

7

- Pairwise energy density

$$\mathcal{W}^\epsilon(S(\mathbf{y}, \mathbf{x}; \mathbf{u}(t))) = J^\epsilon(|\mathbf{y} - \mathbf{x}|) \frac{1}{\epsilon |\mathbf{y} - \mathbf{x}|} \psi(\sqrt{|\mathbf{y} - \mathbf{x}|} S(\mathbf{y}, \mathbf{x}; \mathbf{u}(t)))$$

- State-based energy density $\mathcal{V}^\epsilon(\theta(\mathbf{x}; \mathbf{u}(t))) = \frac{g(\theta(\mathbf{x}; \mathbf{u}(t)))}{\epsilon^2}$

- Total peridynamic energy

$$PD^\epsilon(\mathbf{u}) = \frac{1}{|B_\epsilon(\mathbf{0})|} \int_D \int_{B_\epsilon(\mathbf{x})} |\mathbf{y} - \mathbf{x}| \mathcal{W}^\epsilon(S(\mathbf{y}, \mathbf{x}; \mathbf{u}(t))) \, d\mathbf{y} d\mathbf{x} + \int_D \mathcal{V}^\epsilon(\theta(\mathbf{x}; \mathbf{u}(t))) \, d\mathbf{x}$$

- Lagrangian $L(\mathbf{u}, \dot{\mathbf{u}}, t) = \frac{\rho}{2} \|\dot{\mathbf{u}}\|_{L^2(D; \mathbb{R}^d)}^2 - PD^\epsilon(\mathbf{u}) + \int_D \mathbf{b} \cdot \mathbf{u} \, d\mathbf{x}$

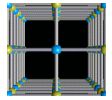
- Applying the principle of least action gives the nonlocal dynamics

$$\rho \ddot{\mathbf{u}}(\mathbf{x}, t) = \mathbf{F}^\epsilon(\mathbf{x}, t) + \mathbf{b}(\mathbf{x}, t), \text{ for } \mathbf{x} \in D$$

- Initial condition $\mathbf{u}(\mathbf{x}, 0) = \mathbf{u}_0(\mathbf{x}), \dot{\mathbf{u}}(\mathbf{x}, 0) = \mathbf{v}_0(\mathbf{x})$

- Boundary condition $\mathbf{u}(\mathbf{x}, t) = \mathbf{0}$ for $\mathbf{x} \in D_c$

- For $\mathbf{b} \in C^1([0, T]; L^\infty(D; \mathbb{R}^d))$ and initial data $\mathbf{u}_0, \mathbf{v}_0 \in L^\infty(D; \mathbb{R}^d)$, solution exist in $C^2([0, T]; L^\infty(D; \mathbb{R}^d))$ **Lipton et al (2018)**



Finite difference approximation

Approximate peridynamic equation using piecewise constant interpolation and central in time discretization. Let \mathbf{u}_i^k denote the discrete displacement at mesh node \mathbf{x}_i and time $t^k = k\Delta t$. We consider following piecewise constant function

$$\mathbf{u}_h^k(\mathbf{x}) = \sum_{i, \mathbf{x}_i \in D} \mathbf{u}_i^k \chi_{U_i}(\mathbf{x})$$

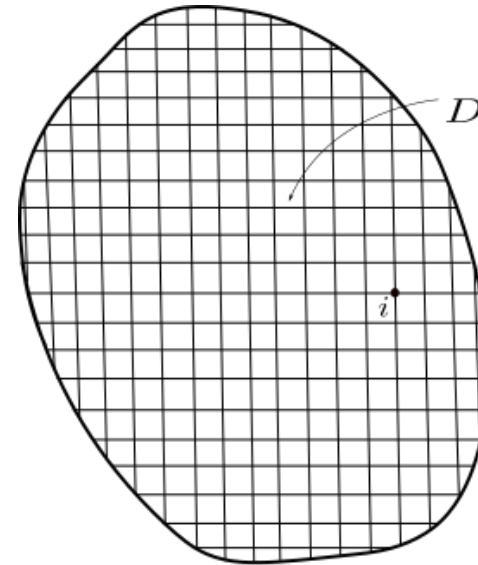
Discrete problem is

$$\frac{\mathbf{u}_h^{k+1} - 2\mathbf{u}_h^k + \mathbf{u}_h^{k-1}}{\Delta t^2} = \mathbf{F}_h(t^k) + \mathbf{b}_h^k,$$

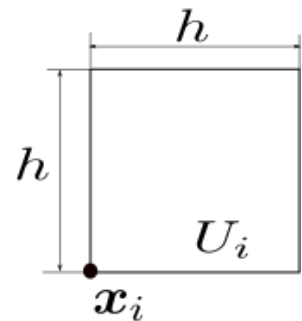
where

$$\mathbf{F}_h(\mathbf{x}, t^k) = \sum_{i, \mathbf{x}_i \in D} \mathbf{F}(\mathbf{x}_i, t^k) \chi_{U_i}(\mathbf{x}),$$

$$\mathbf{b}_h(\mathbf{x}, t^k) = \sum_{i, \mathbf{x}_i \in D} \mathbf{b}(\mathbf{x}_i, t^k) \chi_{U_i}(\mathbf{x})$$



(a)

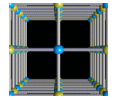


(b)

Writing discrete problem in two first order difference equation

$$\frac{\mathbf{u}_h^{k+1} - \mathbf{u}_h^k}{\Delta t} = \mathbf{v}_h^{k+1}$$

$$\frac{\mathbf{v}_h^{k+1} - \mathbf{v}_h^k}{\Delta t} = \mathbf{F}_h(t^k) + \mathbf{b}_h^k$$



A priori convergence

9

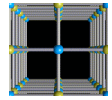
- Well-posedness of solutions in Hölder space $C^{0,\gamma}(D; \mathbb{R}^d)$ and existence of solutions in $C^2([0, T]; C^{0,\gamma}(D; \mathbb{R}^d))$ is shown in **Jha & Lipton (2018a)**

- $E^k := \|\mathbf{u}_h^k - \mathbf{u}(t^k)\| + \|\mathbf{v}_h^k - \mathbf{v}(t^k)\|$

Theorem 1. *Let $\epsilon > 0$ be fixed. Let (\mathbf{u}, \mathbf{v}) be the solution of peridynamic equation. We assume $\mathbf{u}, \mathbf{v} \in C^2([0, T]; C^{0,\gamma}(D; \mathbb{R}^d))$. Then the finite difference scheme is consistent in both time and spatial discretization and converges to the exact solution uniformly in time with respect to the L^2 norm. If we assume the error at the initial step is zero then the error E^k at time t^k is bounded and satisfies*

$$\sup_{0 \leq k \leq T/\Delta t} E^k \leq O \left(C_t \Delta t + C_s \frac{h^\gamma}{\epsilon^2} \right),$$

where constant C_s and C_t are independent of h and Δt and C_s depends on the Hölder norm of the solution and C_t depends on the L^2 norms of time derivatives of the solution.



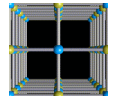
Numerical experiments: Material properties

10

- Pairwise potential: $\psi(r) = c(1 - \exp[-\beta r^2])$
- State-based potential: $g(r) = \bar{C}r^2/2$
- Influence function: $J(r) = 1 - r$ for $0 \leq r < 1$ and $J(r) = 0$ for $r \geq 1$
- Critical strain: $S_c(\mathbf{y}, \mathbf{x}) = \frac{\pm \bar{r}}{\sqrt{|\mathbf{y} - \mathbf{x}|}}$

Parameters \ Poisson's ratio	$\nu = 0.22$	$\nu = 0.245$
c	4712.4	4712.4
\bar{C}	-1.0623×10^{12}	-1.7349×10^{11}
β	1.7533×10^8	1.5647×10^8
\bar{r}	5.3402×10^{-5}	5.6529×10^{-5}

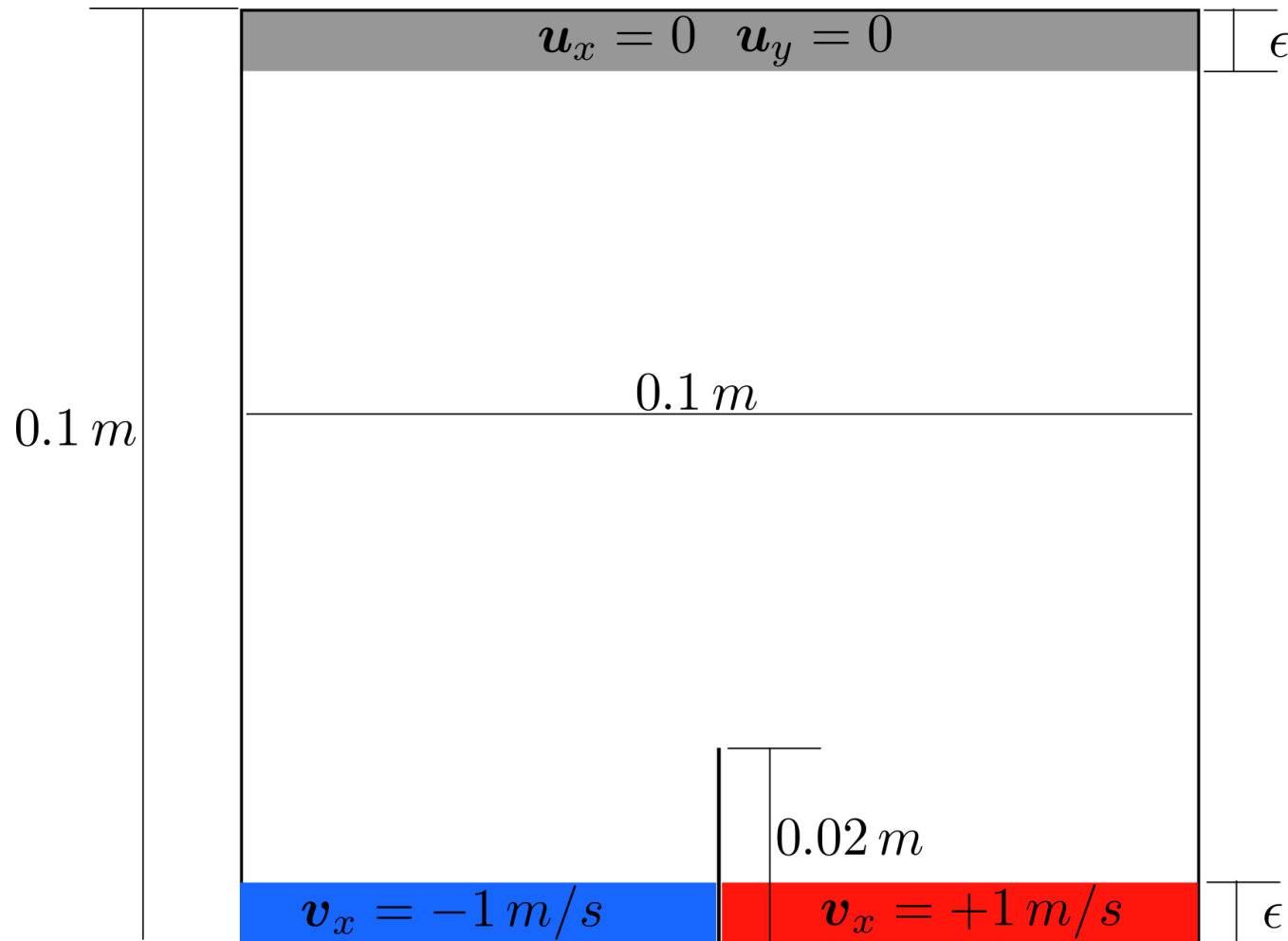
Table 1: Peridynamic material parameters assuming bulk modulus $K = 25$ GPa and critical energy release rate $G_c = 500$ J/m². Density is $\rho = 1200$ kg/m³. Relation between peridynamic parameters and elastic constant and G_c is established in **Lipton et al (2018)**.

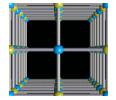


Mode I crack propagation: Setup

11

- Poisson's ratio: $\nu = 0.245$
- Final time $T = 34\mu s$, time step $\Delta t = 0.004\mu s$
- Uniform grid on square domain $D = [0, 0.1 m]^2$



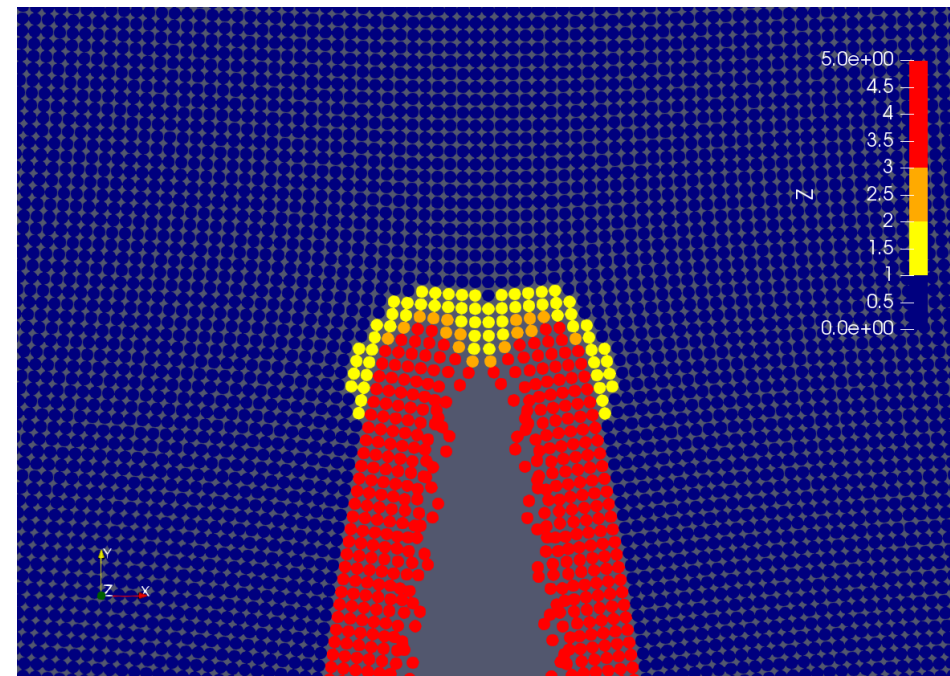
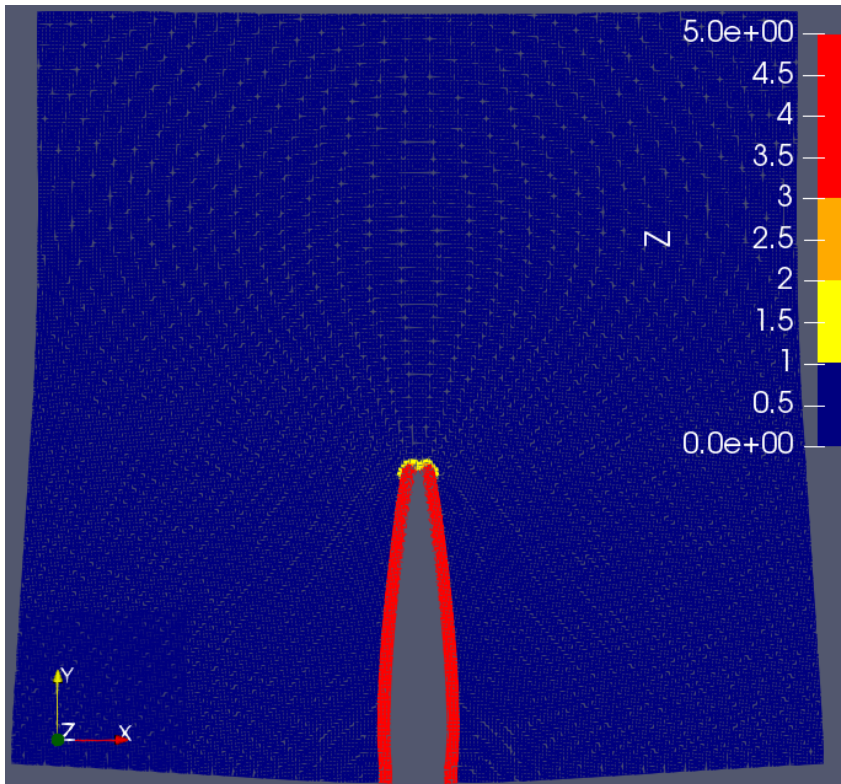


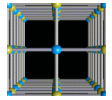
Mode I crack propagation: Damage profile

12

- Horizon $\epsilon = 4$ mm, mesh size $h = 1$ mm
- To measure the extent of damage at material point \mathbf{x} we consider function $Z(\mathbf{x})$ given by

$$Z(\mathbf{x}) = \max_{\mathbf{y} \in H_\epsilon(\mathbf{x}) \cap D} \frac{S(\mathbf{y}, \mathbf{x}; \mathbf{u})}{S_c}$$





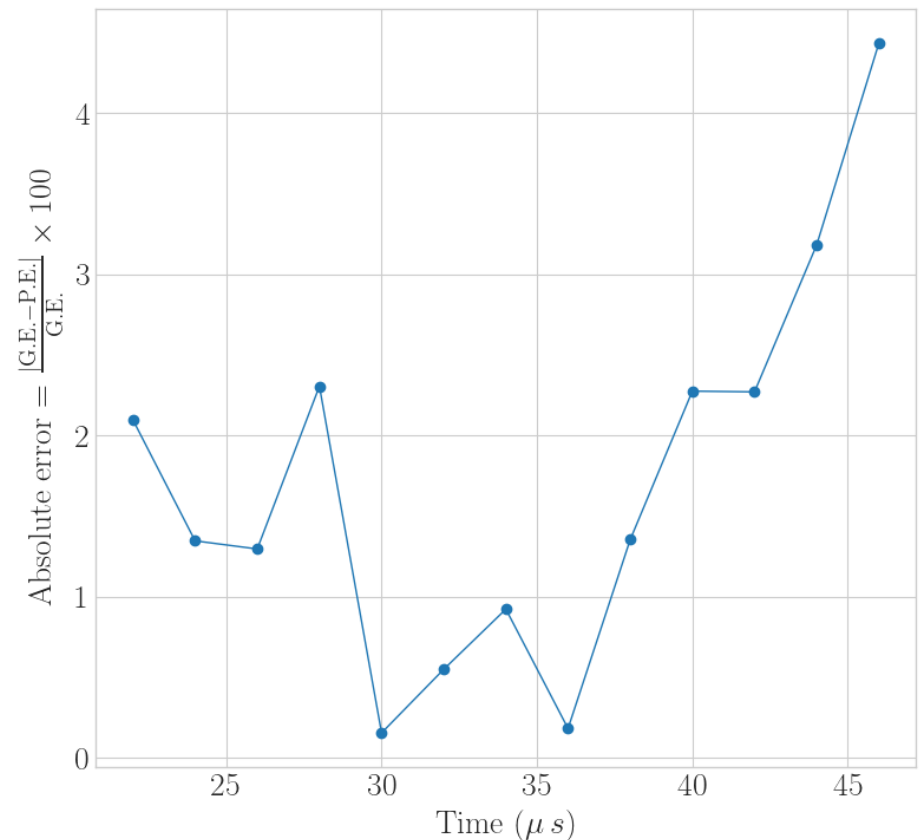
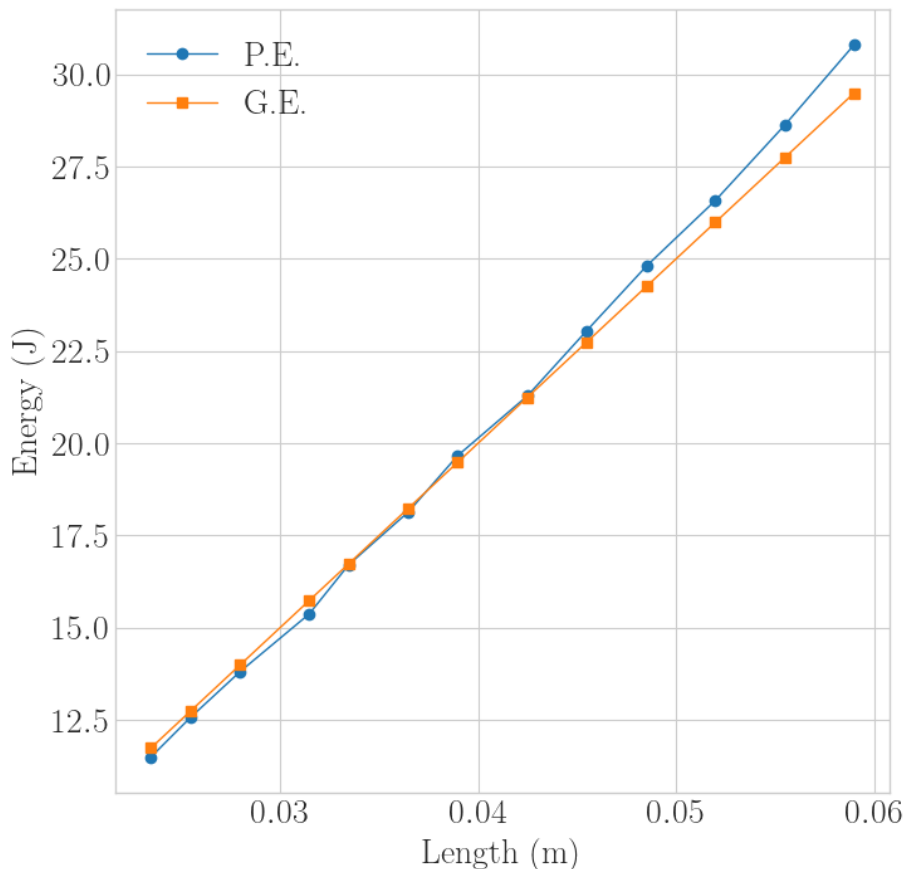
Mode I crack propagation: Fracture energy

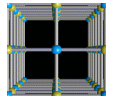
13

- We define the crack zone as set of material points which have $Z > 1$. For a crack of length l , the Griffith's fracture energy (G.E.) will be $G.E. = G_c \times l$. The peridynamic fracture energy (P.E.) is given by

$$P.E. = \int_{\substack{\mathbf{x} \in D, \\ Z(\mathbf{x}) \geq 1}} \left[\frac{1}{\epsilon^d \omega_d} \int_{H_\epsilon(\mathbf{x})} |\mathbf{y} - \mathbf{x}| \mathcal{W}^\epsilon(S(\mathbf{y}, \mathbf{x}, \mathbf{u})) \, d\mathbf{y} \right] d\mathbf{x},$$

where $\mathcal{W}^\epsilon(S(\mathbf{y}, \mathbf{x}, \mathbf{u}))$ is the bond-based potential.

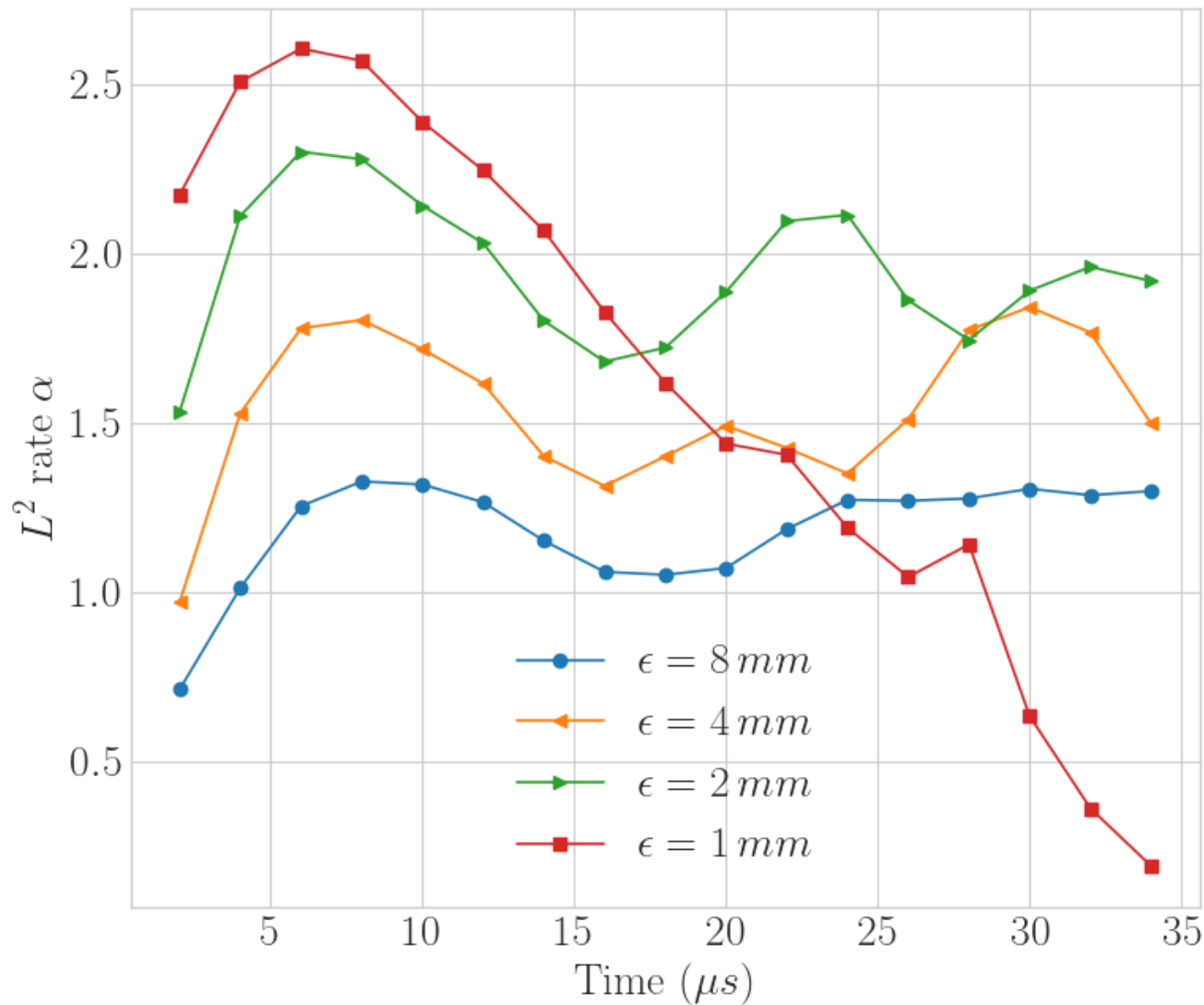


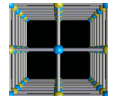


Mode I crack propagation: Convergence rate

14

- For each horizon in 8, 4, 2, 1 mm, we obtain numerical results for three mesh sizes $h = \epsilon/2, \epsilon/4, \epsilon/8$ and compute the rate of convergence

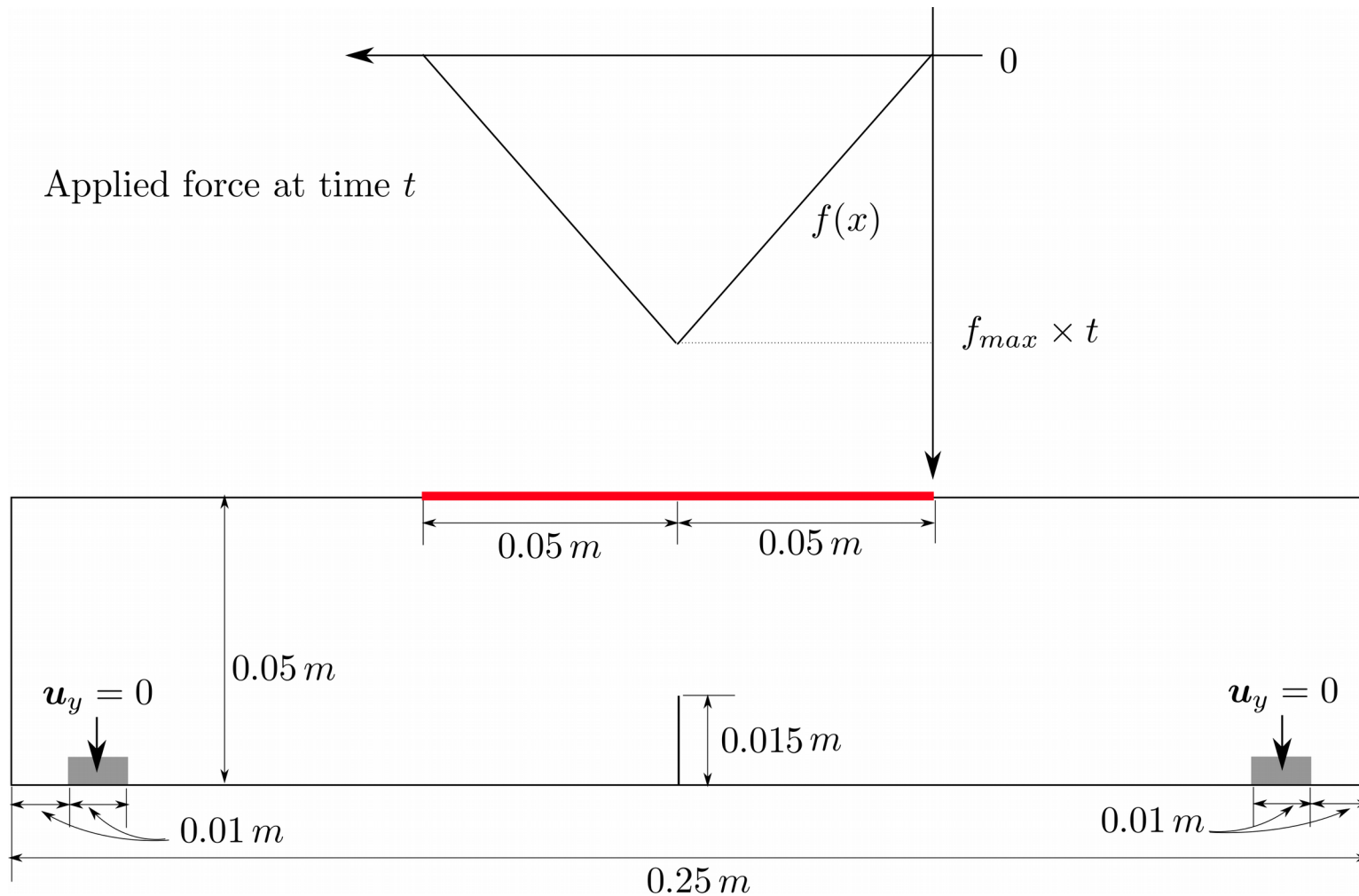


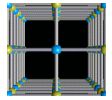


Specimen with pre-crack under bending load

15

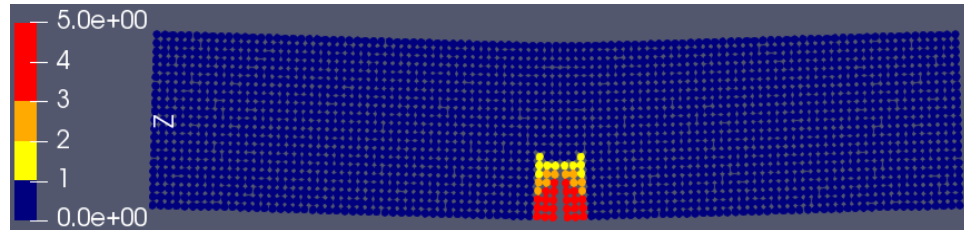
- Poisson's ratio: $\nu = 0.22$
- Final time $T = 350\mu s$, time step $\Delta t = 0.0014\mu s$
- Uniform grid on rectangle domain $D = [0, 0.25\text{ m}] \times [0, 0.05\text{ m}]$



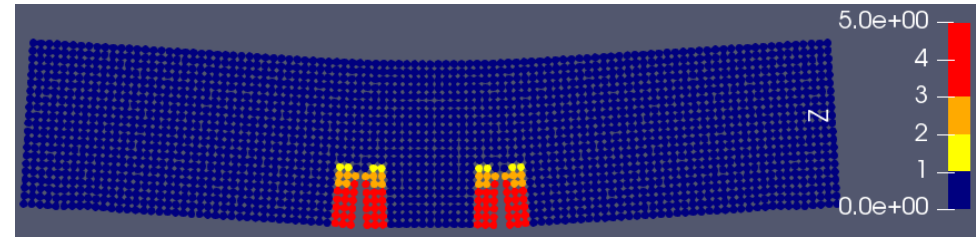


Specimen with pre-crack under bending load

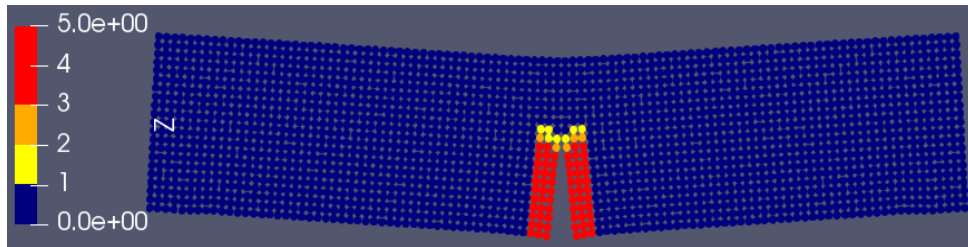
16



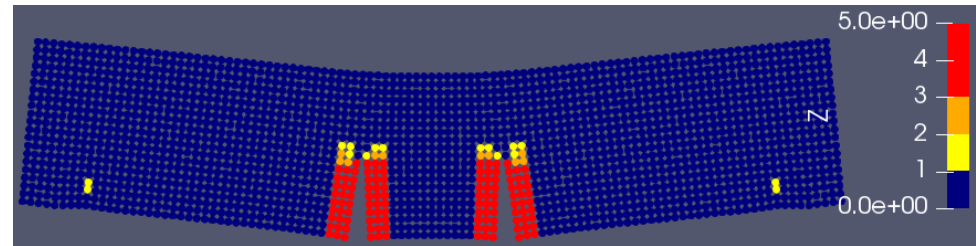
$t = 130 \mu s$



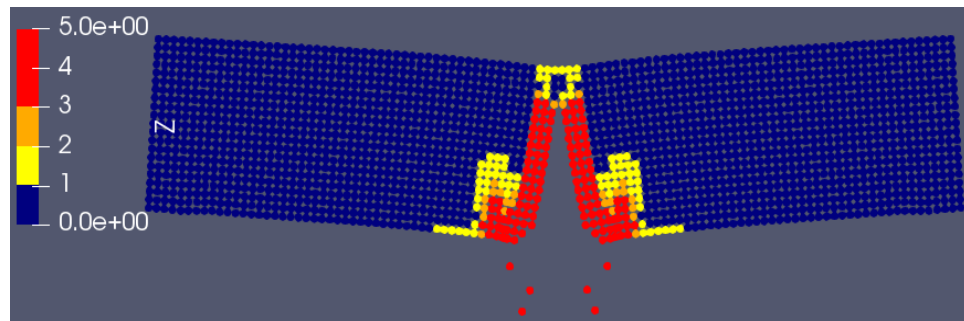
$t = 180 \mu s$



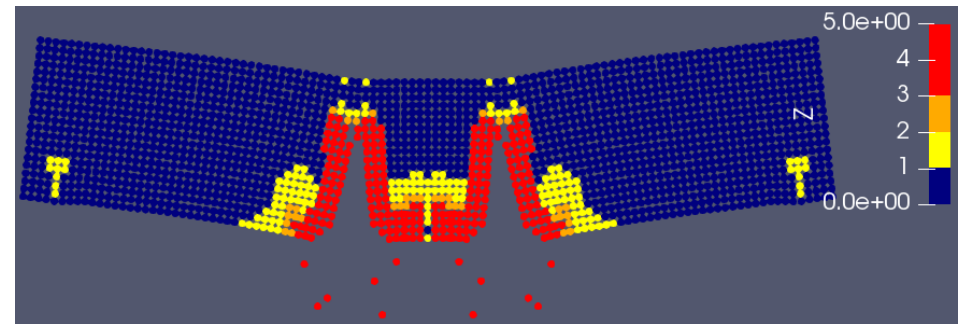
$t = 180 \mu s$



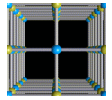
$t = 220 \mu s$



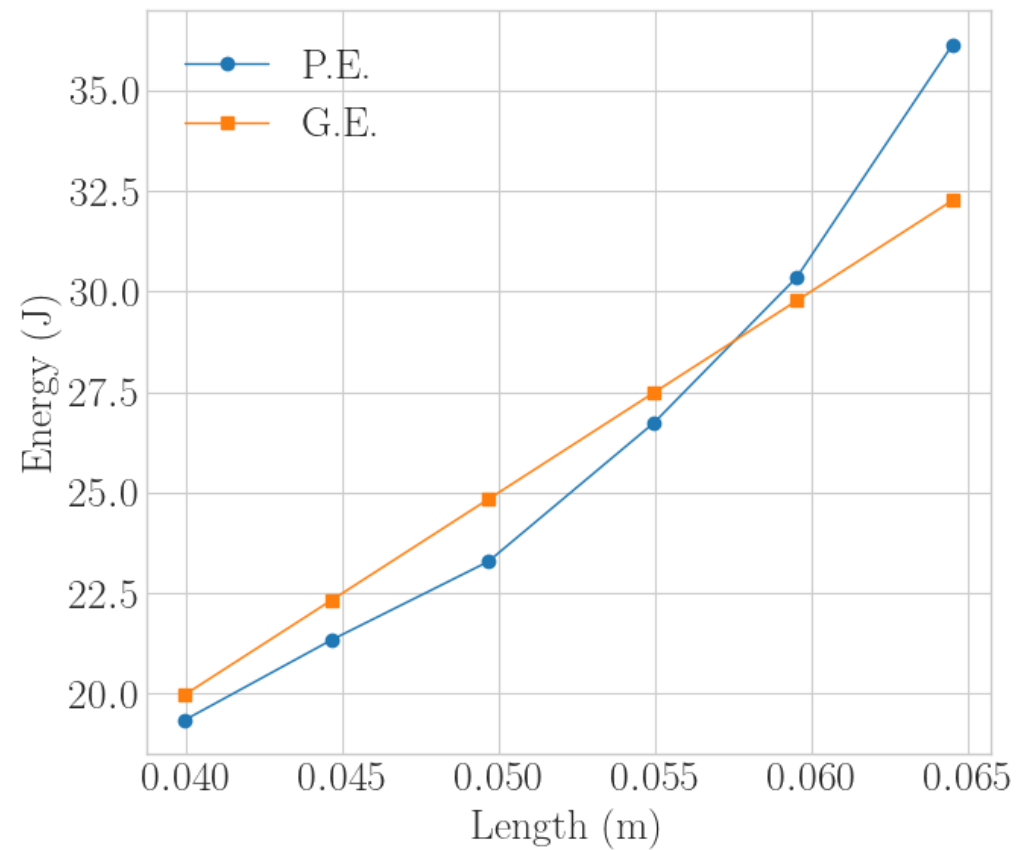
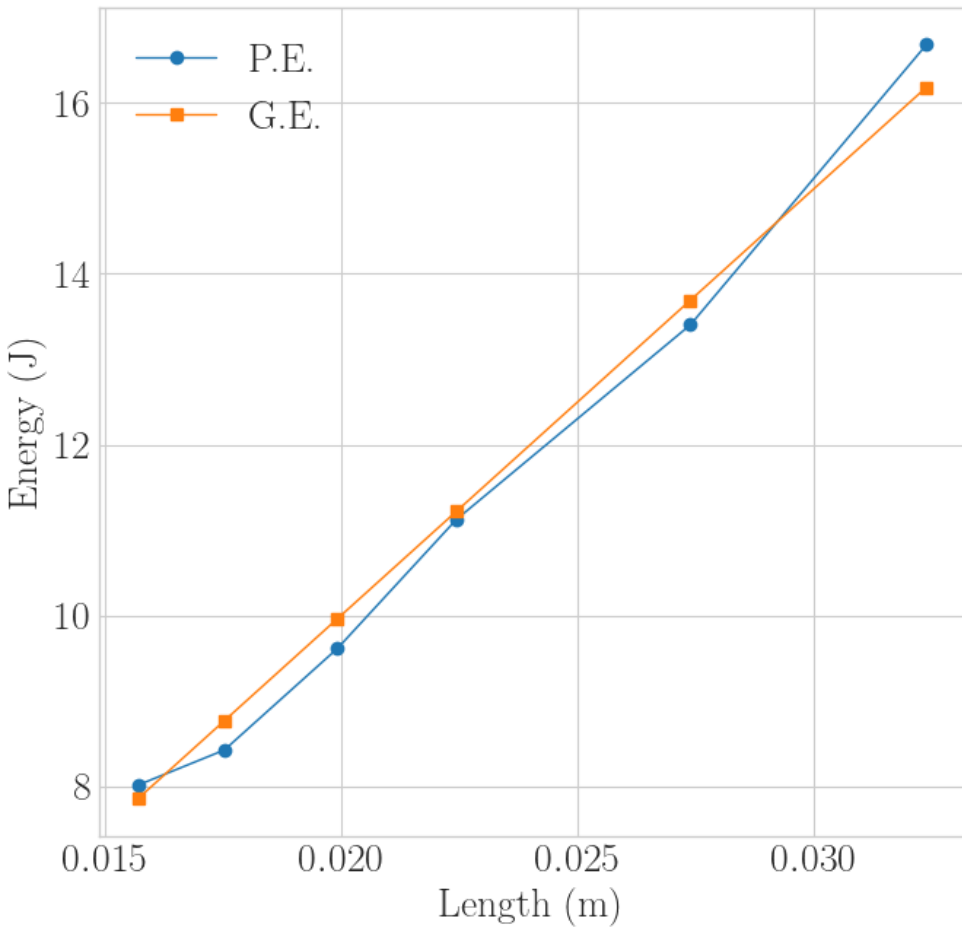
$t = 190 \mu s$

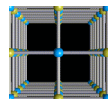


$t = 240 \mu s$



Specimen with pre-crack under bending load





Finite element approximation

18

Let V_h is given by linear continuous interpolations over tetrahedral or triangular elements \mathcal{T}_h where h denotes the size of finite element mesh. Here we assume the elements are conforming and the finite element mesh is shape regular and $V_h \subset H_0^1(D; \mathbb{R}^d)$.

For a continuous function \mathbf{u} on \bar{D} , $\mathcal{I}_h(\mathbf{u})$ is the continuous piecewise linear interpolant on \mathcal{T}_h . It is given by

$$\mathcal{I}_h(\mathbf{u}) \Big|_{\mathsf{T}} = \mathcal{I}_{\mathsf{T}}(\mathbf{u}) \quad \forall \mathsf{T} \in \mathcal{T}_h,$$

where $\mathcal{I}_{\mathsf{T}}(\mathbf{u})$ is the local interpolant defined over finite element T and is given by

$$\mathcal{I}_{\mathsf{T}}(\mathbf{u}) = \sum_{i=1}^n \mathbf{u}(\mathbf{x}_i) \phi_i.$$

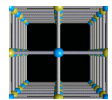
Here n is the number of vertices in an element T , \mathbf{x}_i is the position of vertex i , and ϕ_i is the linear interpolant associated to vertex i .

Let $\mathbf{r}_h(\mathbf{u})$ denote the projection of $\mathbf{u} \in H_0^1(D; \mathbb{R}^d)$ on V_h . For the L^2 norm it is defined as

$$\|\mathbf{u} - \mathbf{r}_h(\mathbf{u})\| = \inf_{\tilde{\mathbf{u}} \in V_h} \|\mathbf{u} - \tilde{\mathbf{u}}\|.$$

and satisfies

$$(\mathbf{r}_h(\mathbf{u}), \tilde{\mathbf{u}}) = (\mathbf{u}, \tilde{\mathbf{u}}), \quad \forall \tilde{\mathbf{u}} \in V_h$$



Central difference time discretization

19

$(\mathbf{u}_h^k, \mathbf{v}_h^k)$ and $(\mathbf{u}^k, \mathbf{v}^k)$ denote the approximate and the exact solution at k^{th} step. Projection is denoted as $(\mathbf{r}_h(\mathbf{u}^k), \mathbf{r}_h(\mathbf{v}^k))$. Approximate initial condition $\mathbf{u}_0, \mathbf{v}_0$ by their projection $\mathbf{r}_h(\mathbf{u}_0), \mathbf{r}_h(\mathbf{v}_0)$ and set $\mathbf{u}_h^0 = \mathbf{r}_h(\mathbf{u}_0), \mathbf{v}_h^0 = \mathbf{r}_h(\mathbf{v}_0)$.

For $k \geq 1$, $(\mathbf{u}_h^k, \mathbf{v}_h^k)$ satisfies, for all $\tilde{\mathbf{u}} \in V_h$,

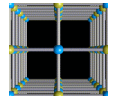
$$\begin{aligned} \left(\frac{\mathbf{u}_h^{k+1} - \mathbf{u}_h^k}{\Delta t}, \tilde{\mathbf{u}} \right) &= (\mathbf{v}_h^{k+1}, \tilde{\mathbf{u}}), \\ \left(\frac{\mathbf{v}_h^{k+1} - \mathbf{v}_h^k}{\Delta t}, \tilde{\mathbf{u}} \right) &= (\mathbf{F}^\epsilon(t^k), \tilde{\mathbf{u}}) + (\mathbf{b}_h^k, \tilde{\mathbf{u}}), \end{aligned}$$

where we denote projection of $\mathbf{b}(t^k), \mathbf{r}_h(\mathbf{b}(t^k))$, as \mathbf{b}_h^k . Combining the two equations delivers central difference equation for \mathbf{u}_h^k . We have

$$\left(\frac{\mathbf{u}_h^{k+1} - 2\mathbf{u}_h^k + \mathbf{u}_h^{k-1}}{\Delta t^2}, \tilde{\mathbf{u}} \right) = (\mathbf{F}^\epsilon(t^k), \tilde{\mathbf{u}}) + (\mathbf{b}_h^k, \tilde{\mathbf{u}}), \quad \forall \tilde{\mathbf{u}} \in V_h.$$

For $k = 0$, we have $\forall \tilde{\mathbf{u}} \in V_h$

$$\left(\frac{\mathbf{u}_h^1 - \mathbf{u}_h^0}{\Delta t^2}, \tilde{\mathbf{u}} \right) = \frac{1}{2}(\mathbf{f}^\epsilon(\mathbf{u}_h^0), \tilde{\mathbf{u}}) + \frac{1}{\Delta t}(\mathbf{v}_h^0, \tilde{\mathbf{u}}) + \frac{1}{2}(\mathbf{b}_h^0, \tilde{\mathbf{u}}).$$



A priori convergence

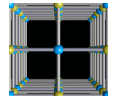
20

- Well-posedness of solutions in $H^2(D; \mathbb{R}^d) \cap H_0^1(D; \mathbb{R}^d)$ space and existence of $C^2([0, T]; H^2(D; \mathbb{R}^d) \cap H_0^1(D; \mathbb{R}^d))$ is shown in **Jha & Lipton (2018b)**
- $E^k := \|\mathbf{u}_h^k - \mathbf{u}(t^k)\| + \|\mathbf{v}_h^k - \mathbf{v}(t^k)\|$

Theorem 2. *Let $\epsilon > 0$ be fixed. Let (\mathbf{u}, \mathbf{v}) be the solution of peridynamic equation. We assume $\mathbf{u}, \mathbf{v} \in C^2([0, T]; H^2(D; \mathbb{R}^d) \cap H_0^1(D; \mathbb{R}^d))$. Then the finite difference scheme is consistent in both time and spatial discretization and converges to the exact solution uniformly in time with respect to the L^2 norm. If we assume the error at the initial step is zero then the error E^k at time t^k is bounded and satisfies*

$$\sup_{0 \leq k \leq T/\Delta t} E^k \leq O\left(C_t \Delta t + C_s \frac{h^2}{\epsilon^2}\right),$$

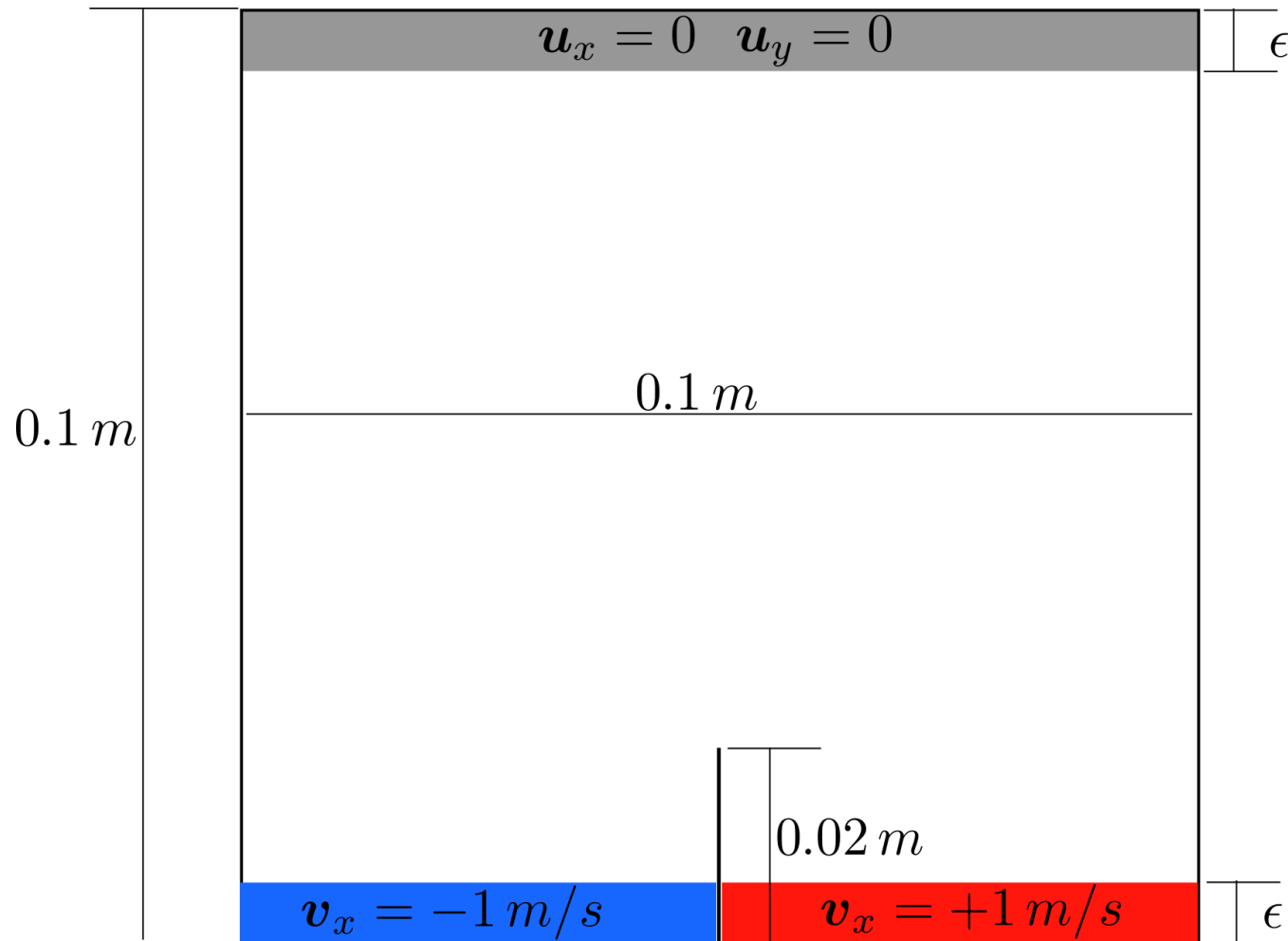
where constant C_s and C_t are independent of h and Δt and C_s depends on the H^2 norm of the solution and C_t depends on the L^2 norms of time derivatives of the solution.

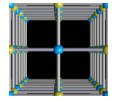


Mode I crack propagation: Setup

21

- Poisson's ratio: $\nu = 0.245$
- Final time $T = 40\mu s$, time step $\Delta t = 0.004\mu s$
- Uniform grid on square domain $D = [0, 0.1 m]^2$



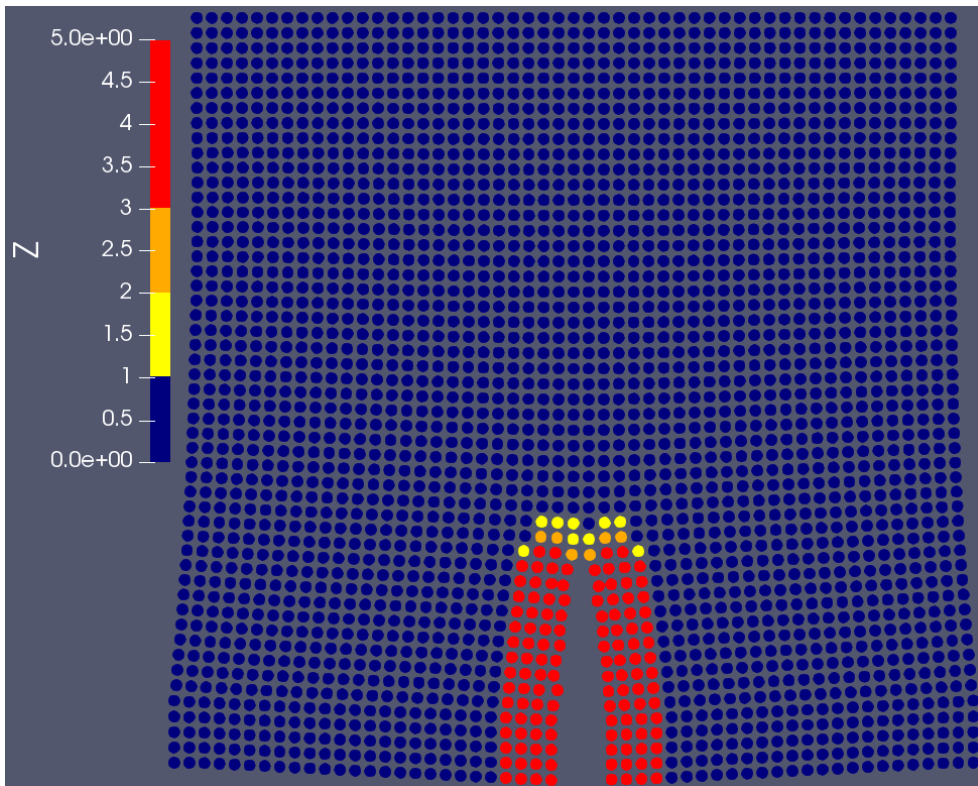


Mode I crack propagation: Damage profile

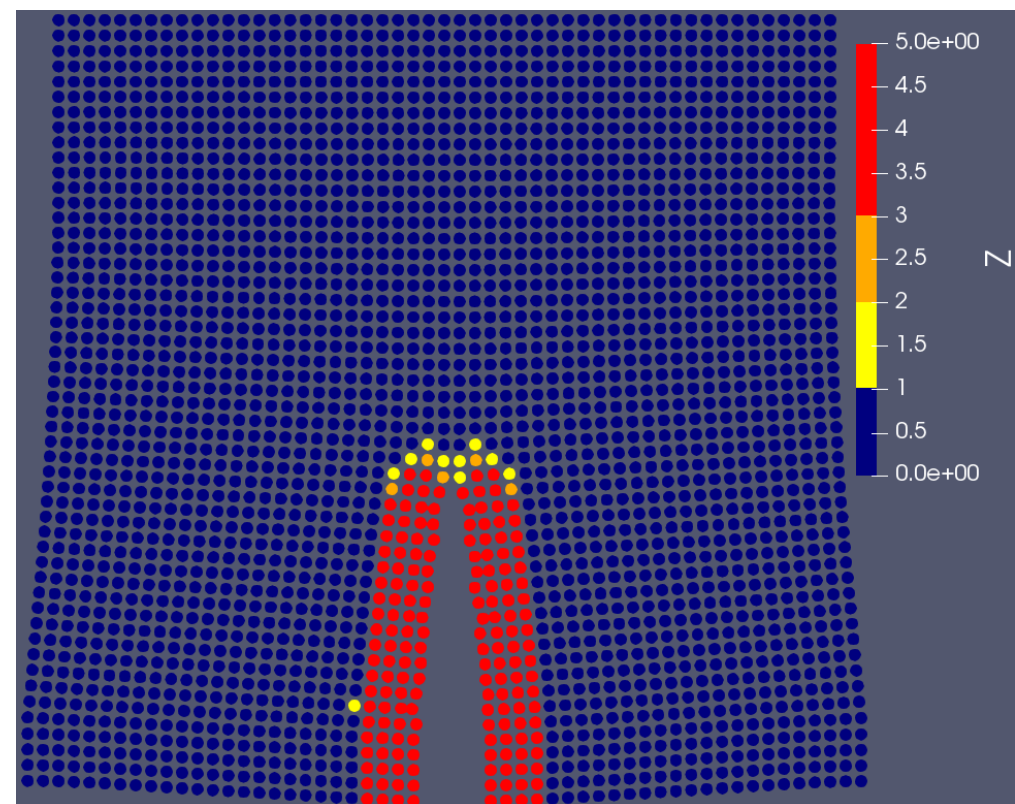
22

- Horizon $\epsilon = 8$ mm, mesh size $h = 2$ mm
- To measure the extent of damage at material point \mathbf{x} we consider function $Z(\mathbf{x})$ given by

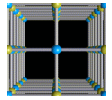
$$Z(\mathbf{x}) = \max_{\mathbf{y} \in H_\epsilon(\mathbf{x}) \cap D} \frac{S(\mathbf{y}, \mathbf{x}; \mathbf{u})}{S_c}$$



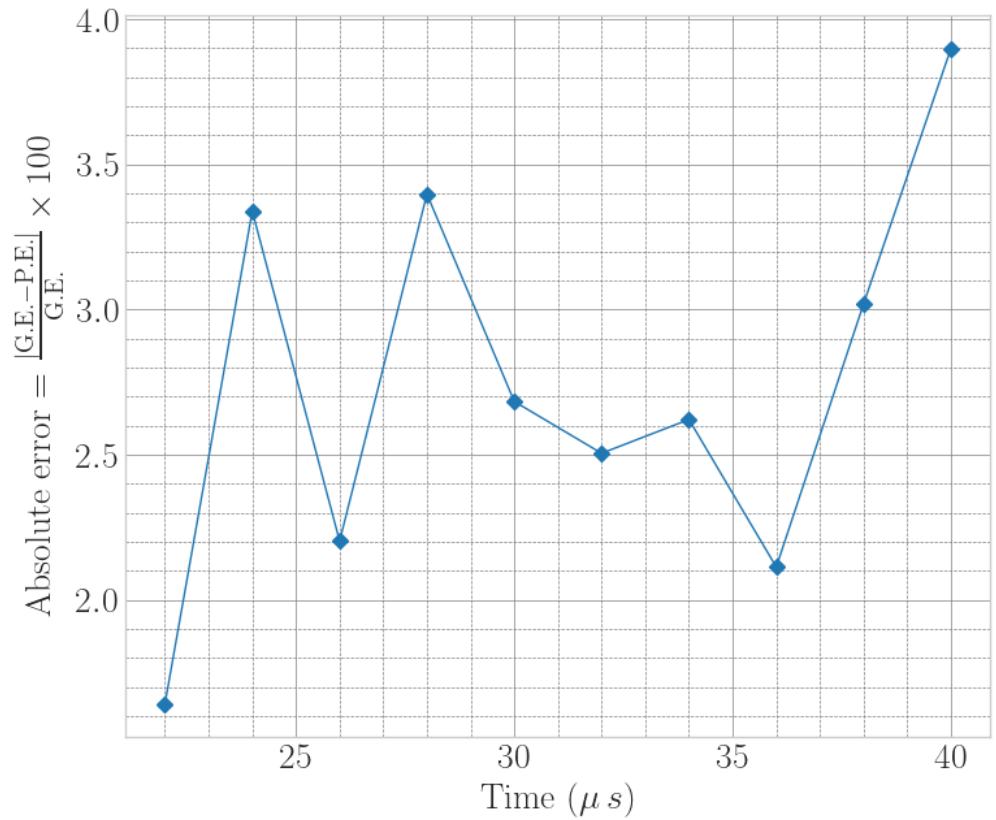
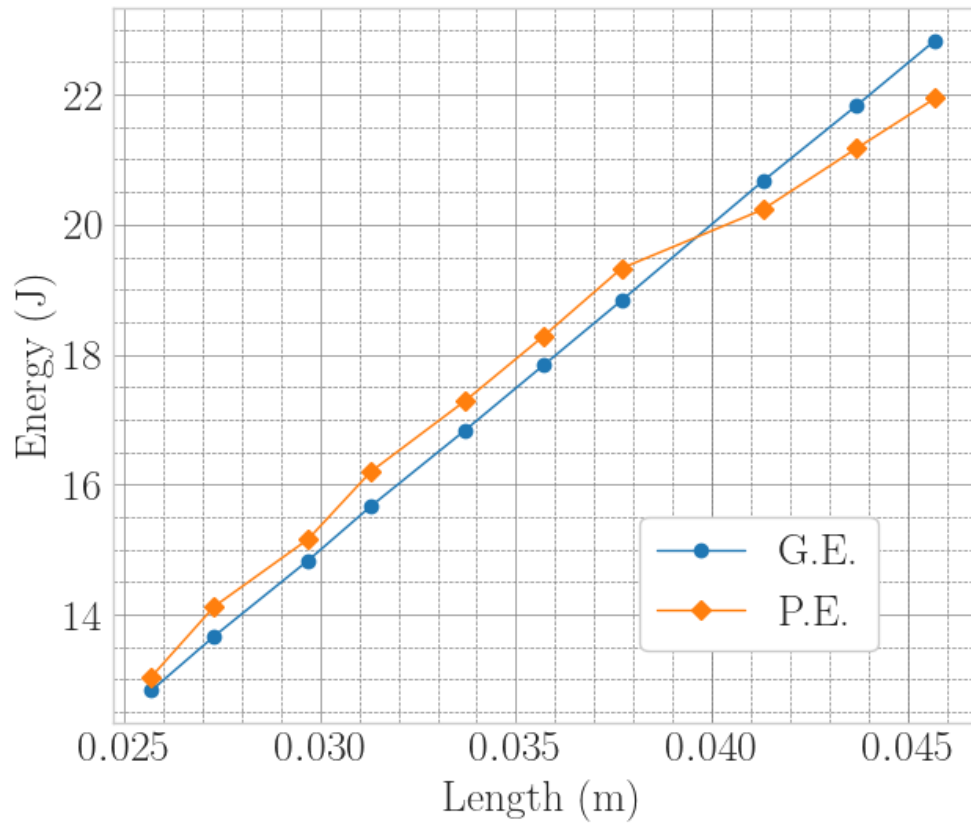
$t = 30 \mu s$

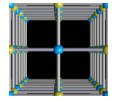


$t = 40 \mu s$



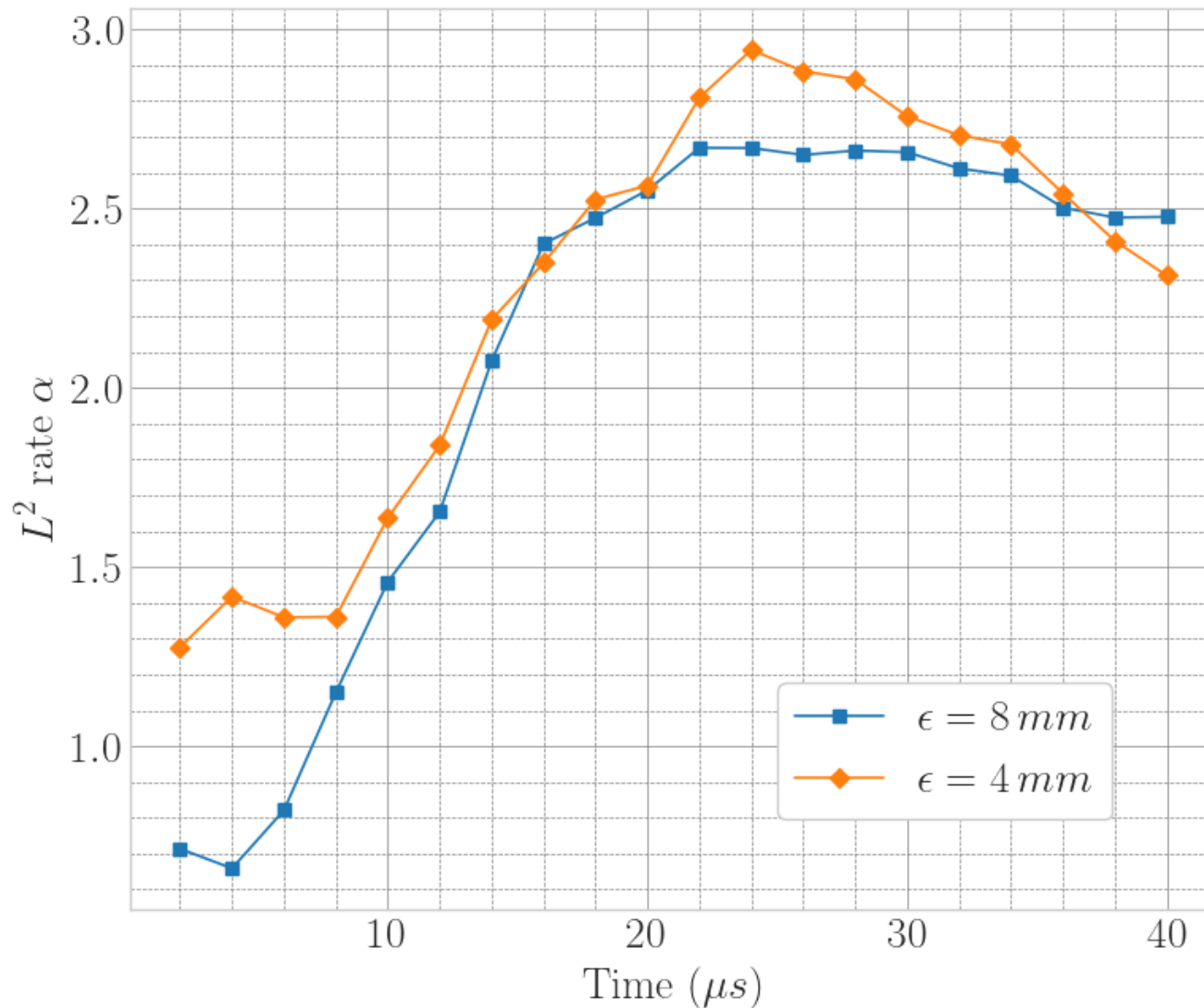
Mode I crack propagation: Fracture energy

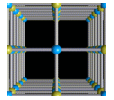




Mode I crack propagation: Convergence rate

- For each 8 mm and 4 mm horizon, we obtain numerical results for three mesh sizes $h = 2, 1, 0.5$ mm and compute the rate of convergence

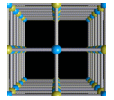




Summary

25

- Numerical analysis of state-based peridynamics model.
- Well-posedness of evolutions in appropriate spaces for error estimates.
- Implementation of finite difference and finite element approximation.
- Good agreement between a priori rate and numerical convergence rate for both finite difference and finite element approximation.
- Peridynamic fracture energy is shown to be close to Griffith's fracture energy for mode I crack propagation.



Future works

26

- Comparison between peridynamics model (in Quasistatic setting) and phase field models.
- Coupling of local and nonlocal models to reduce computational time and memory consumption.
- 3-d implementation of peridynamic code.

Thank you!